

Photometry of Magellanic Cloud clusters with the Advanced Camera for Surveys - I. The old LMC clusters NGC 1928, 1939 and Reticulum

A. D. Mackey^{1*} and G. F. Gilmore¹

¹*Institute of Astronomy, University of Cambridge, Madingley Road, Cambridge CB3 0HA*

Accepted –. Received –

ABSTRACT

We present the results of photometric measurements from images of the LMC globular clusters NGC 1928, 1939 and Reticulum taken with the Advanced Camera for Surveys on the *Hubble Space Telescope*. Exposures through the F555W and F814W filters result in high accuracy colour-magnitude diagrams (CMDs) for these three clusters. This is the first time that CMDs for NGC 1928 and 1939 have been published. All three clusters possess CMDs with features indicating them to be > 10 Gyr old, including main sequence turn-offs at $V \sim 23$ and well populated horizontal branches (HBs). We use the CMDs to obtain metallicity and reddening estimates for each cluster. NGC 1939 is a metal-poor cluster, with $[\text{Fe}/\text{H}] = -2.10 \pm 0.19$, while NGC 1928 is significantly more metal-rich, with $[\text{Fe}/\text{H}] = -1.27 \pm 0.14$. The abundance of Reticulum is intermediate between the two, with $[\text{Fe}/\text{H}] = -1.66 \pm 0.12$ – a measurement which matches well with previous estimates. All three clusters are moderately reddened, with values ranging from $E(V - I) = 0.07 \pm 0.02$ for Reticulum and $E(V - I) = 0.08 \pm 0.02$ for NGC 1928, to $E(V - I) = 0.16 \pm 0.03$ for NGC 1939. After correcting the CMDs for extinction we estimate the HB morphology of each cluster. NGC 1928 and 1939 possess HBs consisting almost exclusively of stars to the blue of the instability strip, with NGC 1928 in addition showing evidence for an extended blue HB. In contrast, Reticulum has an intermediate HB morphology, with stars across the instability strip. Using a variety of dating techniques we show that these three clusters are coeval with each other and the oldest Galactic and LMC globular clusters, to within ~ 2 Gyr. The census of known old LMC globular clusters therefore now numbers 15 plus the unique, somewhat younger cluster ESO121-SC03. The NGC 1939 field contains another cluster in the line-of-sight, NGC 1938. A CMD for this object shows it to be less than ~ 400 Myr old, and it is therefore unlikely to be physically associated with NGC 1939.

Key words: galaxies: star clusters – globular clusters: individual: NGC 1928, NGC 1938, NGC1939, Reticulum – Magellanic Clouds

1 INTRODUCTION

The Large and Small Magellanic Clouds (LMC/SMC) possess extensive systems of rich stellar clusters. These objects exhibit a much wider variety in age, structure, environment and mass than do Galactic clusters, and this, combined with their relatively close proximity, has rendered them central to a surprising number of fields of modern astrophysics – from star and cluster formation, and stellar evolution, to gravitational dynamics, galactic evolution, and distance scale measurements. They are also vital probes and tracers of the chemical and dynamical evolution of the LMC and SMC themselves. It is therefore important to understand how their properties, and in particular their ages and abundances, are distributed.

It has long been known that the LMC, which contains the more numerous cluster system of the two Clouds, houses a small sub-population of extremely ancient objects. Although early studies revealed half a dozen LMC clusters to possess colour-magnitude diagrams (CMDs) with features similar to those of the Galactic globular clusters, it has only been since the advent of the *Hubble Space Telescope* (*HST*) that imaging resolution and sensitivity has been sufficiently high as to allow accurate colour-magnitude diagrams (CMDs) suitable for relative age dating. A number of relatively recent studies have demonstrated that the number of LMC clusters coeval with each other and the oldest Galactic globular clusters is somewhat more than a dozen – NGC 1466, NGC 2257, and Hodge 11 (e.g., Johnson et al. (1999)); NGC 1754, 1835, 1898, 1916, 2005, and 2019 (e.g., Olsen et al. (1998)); and NGC 1786, 1841 and 2210 (e.g., Brocato et al. (1996)). Several published CMDs

* E-mail: dmackey@ast.cam.ac.uk

show the remote outer cluster Reticulum to be very old (Johnson et al. 1999; Marconi et al. 2002; Monelli et al. 2003); however a full age analysis is yet to be published for this cluster. In addition there are two more clusters located in the LMC bar region – NGC 1928 and 1939 – which integrated spectroscopy suggests could be old (Dutra et al. 1999), but which are so compact and lie against such highly crowded LMC fields that it has not previously been possible to obtain accurate CMDs for them (see for example, the search for old LMC clusters conducted by Geisler et al. (1997)). The census of old LMC clusters is therefore still incomplete.

We have used the Advanced Camera for Surveys (ACS) on *HST* to obtain images of NGC 1928, 1939, and Reticulum as part of program 9891 – a snapshot survey of 40 LMC and 40 SMC clusters. This program is primarily designed to extend the detailed investigation of Mackey & Gilmore (2003a; 2003b) concerning the structural evolution of Magellanic Cloud clusters. However, the ACS observations are of sufficient quality and resolution as to allow colour-magnitude diagrams (CMDs) to be constructed for NGC 1928 and NGC 1939 for the first time, as well as a high quality CMD for Reticulum. In this paper, we present the results of these observations (Section 2) and the measured colour-magnitude diagrams (Section 3). Abundances and reddenings are derived for each cluster, and it is demonstrated that NGC 1928 and 1939, along with Reticulum, are coeval with both well studied Galactic globular clusters (such as M92, M3 and M5) and other old LMC objects (such as NGC 2257 and Hodge 11) (Section 4).

2 OBSERVATIONS AND DATA REDUCTION

The observations were taken during *HST* Cycle 12 using the ACS Wide Field Channel (WFC). As snapshot targets, the clusters were observed for only one orbit each. This allowed two exposures to be taken per cluster – one through the F555W filter and one through the F814W filter. Details of the individual exposures are listed in Table 1. Exposure durations were 330 s in F555W and 200 s in F814W.

The ACS WFC consists of a mosaic of two 2048×4096 SITE CCDs with a scale of ~ 0.05 arcsec per pixel, and separated by a gap of ~ 50 pixels. Each image therefore covers a field of view (FOV) of approximately 202×202 arcseconds. The clusters were centred at the reference point WFC1, located on chip 1 at position (2072, 1024). This allowed any given cluster to be observed up to a radius $r \sim 150''$ from its centre, while also ensuring the cluster core did not fall near the inter-chip gap.

In order to maximise the efficiency of the limited imaging strategy afforded by a snapshot program, all observations were made with the ACS/WFC GAIN parameter set to 2 rather than the default (GAIN = 1). This allowed the full well depth to be sampled (as opposed to only ~ 75 per cent of the full well depth for GAIN = 1) with only a modest increase in read noise (~ 0.3 e⁻ extra rms), thus increasing the dynamic range of the observations by greater than 0.3 mag. In addition, the second image of each cluster was offset by 2 pixels in both the x and y directions, to help facilitate the removal of hot pixels and cosmic rays. With only two images per cluster, through different filters, it is not possible to completely eliminate the inter-chip gap using such an offset.

Before being made available for retrieval from the STScI archive, all images were passed through the standard ACS/WFC reduction pipeline. This process includes bias and dark subtractions, flatfield division, masking of known bad pixels and columns, and the calculation of photometry header keywords. In addition the

STScI *PyDrizzle* software is used to correct the (significant) geometric distortion present in WFC images. The products obtained from the STScI archive are hence fully calibrated and distortion-corrected images, in units of counts per second.

The F555W images of NGC 1928, 1939, and Reticulum may be seen in Figure 1. Both NGC 1928 and NGC 1939 are extremely compact clusters set against heavily populated background fields, while Reticulum is at the other end of the scale – extremely diffuse with almost no background population evident. A second cluster is visible in the image of NGC 1939, slightly to the lower left of the main cluster. This is another LMC member, NGC 1938 (see Section 4.4 and Figure 8).

For each cluster, photometry was performed on the two images individually, using the DAOPHOT software in IRAF. The detailed procedure was as follows. First the DAOFIND task was used with a detection threshold of 4σ above background to locate all the brightness peaks in each image. The two output lists were matched against each other to find objects falling at identical positions in the two frames. Objects detected in the first image but with no matching counterpart in the second image (and vice versa) were discarded.

Performing this cross-matching was not as simple a task as it might at first appear. Because of the significant geometric distortion present in the ACS/WFC observations, a 2×2 pixel offset in the telescope position (i.e., in the object's position on the detector) between the two exposures does not correspond to a 2×2 pixel offset between the two distortion-corrected images. In fact, the value of the offset is position-dependent in the corrected images. There are at least two possible ways to overcome this. The simplest is to use the header information in each of the two images to overlay a common coordinate system (e.g., J2000.0 (α , δ) coordinates) and match between the lists via a transformation from pixel coordinates to the common coordinate system. However, this procedure is completely dependent on the accuracy of the header information in each of the two datasets and the consistency between them, and we possessed no independent means of verifying this for all the observations. Instead, we preferred a more generally applicable and physically grounded procedure. We applied the distortion models used in *PyDrizzle* to transform the observed F555W positions from the distortion-corrected frame to detector positions (i.e., in the distorted frame). The new coordinates were then subjected to the 2×2 pixel offset and transformed into the F814W distortion-corrected frame. This allowed a direct match against the list of object positions measured by DAOFIND from this frame. Given that the distortion models are accurate to a small fraction of a pixel, a match was defined as the transformed F555W position lying within a 0.8 pixel radius of an F814W position. Experimentation showed this limiting radius to be perfectly adequate across the full WFC field of view.

The model defining the relationship between detector coordinates and distortion-corrected coordinates takes the form of a polynomial transformation:

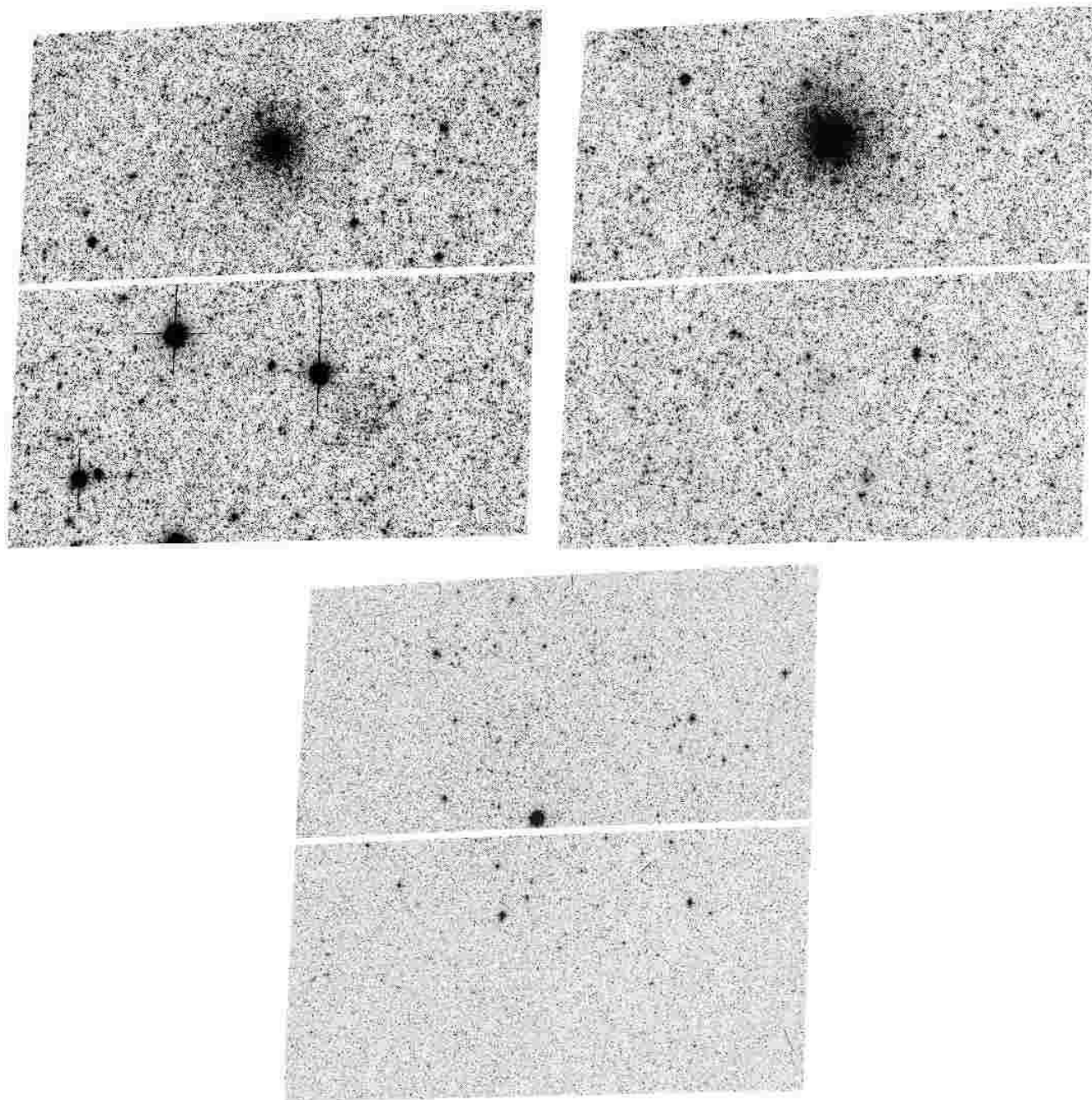
$$x_c = \sum_{i=0}^k \sum_{j=0}^i a_{i,j} (x - x_r)^j (y - y_r)^{i-j} \quad (1)$$

$$y_c = \sum_{i=0}^k \sum_{j=0}^i b_{i,j} (x - x_r)^j (y - y_r)^{i-j} \quad (2)$$

where (x, y) are the detector coordinates (in pixels), (x_c, y_c) are the corrected coordinates (in arcseconds), (x_r, y_r) is the position of a reference pixel, and k is the order of the polynomial. The in-

Table 1. ACS/WFC observations of NGC 1928, 1939, and Reticulum (*HST* program 9891).

Cluster	RA (J2000.0)	Dec. (J2000.0)	Filter	Dataset	Exposure Time (s)	Date
NGC 1928	05 ^h 20 ^m 57.51 ^s	−69° 28′ 41.5″	F555W	j8ne62ztq	330	23/08/2003
			F814W	j8ne62zvq	200	23/08/2003
NGC 1939	05 ^h 21 ^m 26.63 ^s	−69° 56′ 58.2″	F555W	j8ne63ttq	330	27/07/2003
			F814W	j8ne63ttq	200	27/07/2003
Reticulum	04 ^h 36 ^m 09.33 ^s	−58° 51′ 40.3″	F555W	j8ne43a3q	330	21/09/2003
			F814W	j8ne43a7q	200	21/09/2003

**Figure 1.** Distortion-corrected F555W-band ACS/WFC images of NGC 1928 (upper left), NGC 1939 (upper right), and Reticulum (lower). Note the presence of a second cluster (NGC 1938) in the NGC 1939 frame – this object lies to the lower left of the main cluster.

verse transformation takes a similar form. Additional corrections are required to provide a grid common to the two chips which make up the WFC. Full details of the model, including its derivation and application, are provided by Mack et al. (2003). The latest solution may be downloaded from the STScI web site in the form of a matrix of the polynomial coefficients ($a_{i,j}$, etc) along with the required offsets, reference pixel values and plate scales. The version used in the present work was named nar11046j_lidc.

With the cross-matching complete, lists of detected objects were provided to the PHOT task. This was used to perform aperture photometry on each object, using apertures of radius $r = 3$ pixels. We also attempted to use DAOPHOT routines to perform PSF-fitting photometry; however, the quality and internal consistency of the measurements we obtained was not as good as for the aperture photometry. The reasons for this likely have to do with both the nature of the images and of the objects imaged. The PSF is apparently significantly variable across the WFC field of view (possibly due to small imperfections in the distortion correction); while the observations of NGC 1928 and 1939 are extremely crowded (we measured more than 10^5 detections in each field), meaning that it is difficult to find suitable stars to construct model PSFs across the entire field of view. The 3 pixel aperture photometry radius is large enough to be relatively insensitive to PSF variations and small enough to be usable given the crowding, so is an acceptable compromise.

The resultant photometry has been calculated in the STmag system, defined as $m = -2.5 \log_{10} f_\lambda - 21.1$, where f_λ is the flux density per unit wavelength, and the zero-point is set so that Vega has magnitude 0 in the Johnson V passband. The constants required to convert the measured photometry from counts to f_λ were selected from the ACS zero-points web page, and correspond to applying the formula $m = -2.5 \log_{10}(\text{counts s}^{-1}) + ZP$, where $ZP = 25.672$ for the F555W filter and $ZP = 26.776$ for the F814W filter.

Like all previous *HST* CCD instruments, the ACS/WFC chips are suffering from degradation of their charge transfer efficiency (CTE) due to radiation damage. Since ACS is a relatively new instrument, this degradation is not yet large. Nonetheless, photometric measurements already require correction to account for lost flux from imperfect CTE. A calibration of the losses due to parallel (y -direction) CTE effects for ACS/WFC has been provided by Riess (2003), who parametrizes the necessary correction by:

$$\Delta_Y = 10^A \times s^B \times f^C \times \frac{Y}{2048} \times \frac{(MJD - 52333)}{(52714 - 52333)} \text{ mag} \quad (3)$$

where the object's sky (s) and flux (f) values are in counts, Y represents the number of parallel transfers (so if the object has position (x, y) , then $Y = y$ for $1 \leq y \leq 2048$ and $Y = 4096 - y$ for $y > 2048$), and MJD is the Modified Julian Date of the observation being corrected. The Riess calibration provides exponents $A = 0.45 \pm 0.10$, $B = -0.11 \pm 0.03$ and $C = -0.65 \pm 0.04$ for aperture photometry measurements with radius $r = 3$ pixels. At present there appear to be no additional corrections required for serial (x -direction) transfer.

With the CTE corrections calculated, the final step was to determine aperture corrections for each of the measured images. In principle it is desirable to correct to an infinite aperture; however, this was not possible here since no standard stars were observed in our images. Alternatively, it is common to correct to a set aperture, after which a transformation which includes correction to an infinite aperture is often applied to the measurements to place them on a standard magnitude scale (e.g., to move from F555W flight magnitudes to standard Johnson V magnitudes). At the time of

writing however, no such transformations are yet available for the ACS/WFC filter system. Nonetheless, it has become common practise for WFPC2 measurements to correct to an aperture of radius $0.5''$ as prescribed by Holtzman et al. (1995). We therefore calculated a correction to this aperture (10 ACS/WFC pixels) for the present photometry. It is important to note that the aperture correction does not affect the relative photometry for a given cluster since it is applied uniformly across each set of measurements. It is in general important only for placing the photometry on an absolute scale. As an indication of the systematic absolute error, the energy encirclement plots provided by Mack et al. (2003) show that just under 95 per cent of the flux of a point source is contained within $0.5''$ radius. Once suitable transformations for ACS/WFC photometry have been published, it will be a simple procedure to re-calculate the corrections to the required aperture and convert to a standard magnitude system.

Aperture stars were selected according to strict criteria: they must be bright stars but significantly below saturation; they must not have unusual shape characteristics (see Section 3); they must have no neighbouring stars, bad pixels, or image edges within a radius of $1''$; and they must not lie in an area of unusually high background (e.g., near the centre of a cluster). For NGC 1928 and 1939 these criteria defined a set of several hundred stars per image, while for Reticulum the set numbered approximately 100 stars. The photometry procedure described above was repeated on these star lists using apertures of radius 10 pixels, and the mean aperture correction for each image calculated using a 3σ clipping algorithm. Standard errors in the calculated corrections were typically ~ 0.01 mag.

3 COLOUR-MAGNITUDE DIAGRAMS

Colour-magnitude diagrams for the three clusters are presented in Fig. 2. These diagrams show all matched detections – there has been no selection of objects according to shape characteristics (see below). It is clear that the diagrams for NGC 1928 and 1939 are dominated by field stars, as expected. NGC 1928 lies against a somewhat denser field than NGC 1939. Without some form of statistical subtraction, it is impossible to determine which parts of these two CMDs belong to the clusters. The NGC 1939 field suffers in addition from severe differential reddening, as is evident from the smearing of the red clump. In contrast, the CMD for Reticulum is well defined and contains little or no field contamination. The narrowness of the sequences visible in all three CMDs (e.g., the red-giant branches) clearly demonstrate the high internal accuracy of the photometry and the validity of the reduction procedure described in the previous Section.

3.1 Field Star Subtraction

While the CMD for Reticulum clearly possesses little or no field star contamination, statistical subtraction of the field population was absolutely necessary before any study of NGC 1928 and NGC 1939 could be made. For such severely contaminated clusters, statistical subtraction is not a trivial matter. We developed two different subtraction methods and combined the results of each.

The first stage was to remove objects with unusual or non-stellar shape characteristics. Photometry for such objects is likely to be compromised (e.g., by a cosmic ray strike, bad pixel, or the blend of two or more very close stars), or the objects are likely to be background galaxies. Either way, it is desirable to remove

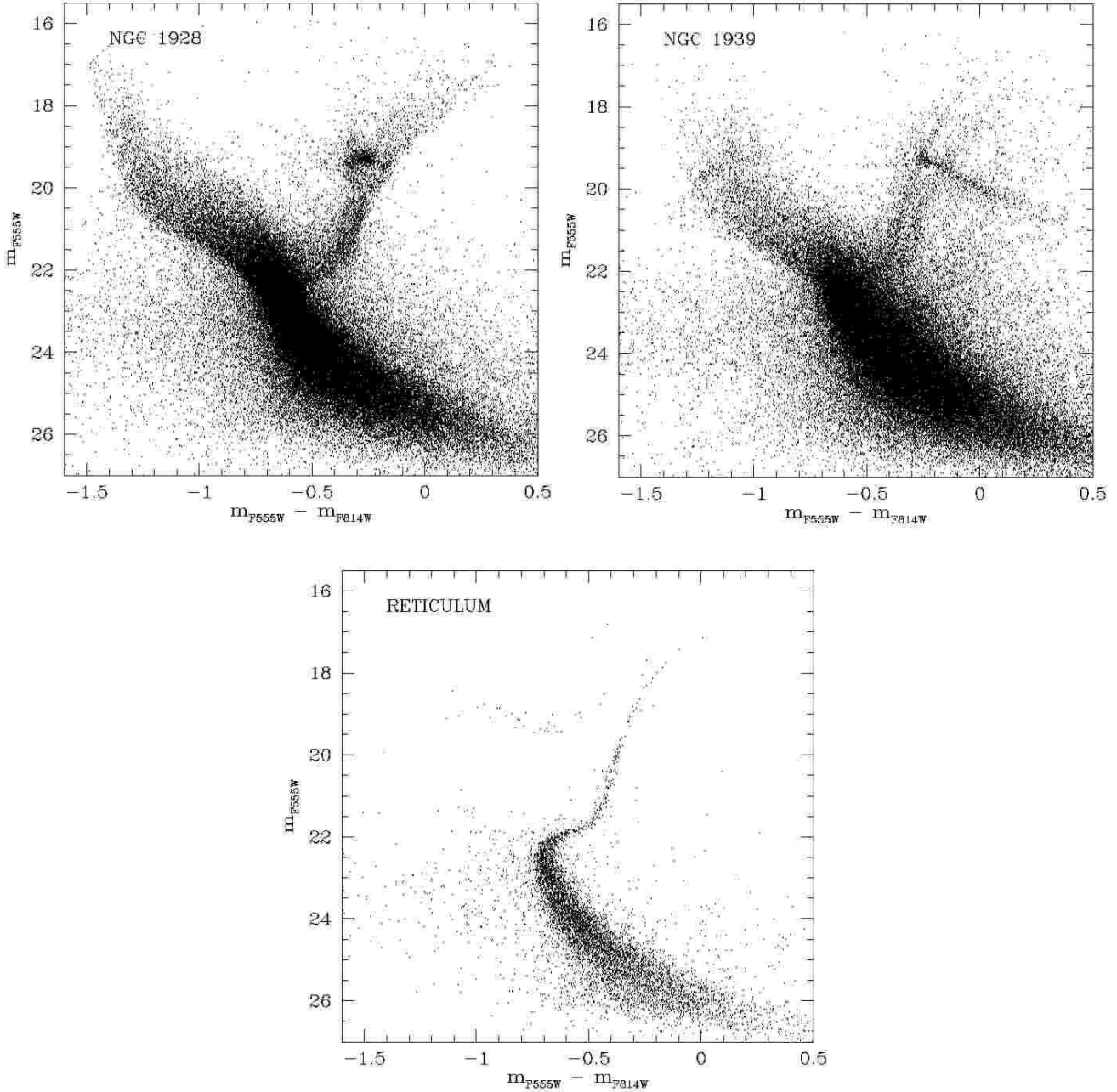


Figure 2. Colour-magnitude diagrams for all detections in each of the three fields. Measurements are plotted in the STmag magnitude system (see text). The CMD for NGC 1928 contains 104 438 detections, while that for NGC 1939 contains 94 546 detections, and the CMD for Reticulum 7 604 detections.

them from the CMDs. The output of the initial detection program, DAOFIND, provided three shape characteristics per detection: a sharpness parameter and two roundness parameters (called *s-round* and *g-round*). The sharpness is a measurement of how high the peak of a detection is relative to a best-fitting Gaussian, while the two roundness parameters are measurements of how circular the object image is. Clean stellar detections should have sharpness ~ 0.75 and round images (roundness parameters ~ 0). For each photometry list we produced histograms of these three parameters in order to determine suitable clipping limits. In general we removed objects which did not have $0.6 < \text{sharpness} < 0.9$ and $-0.35 < \text{roundness} < 0.35$ through both filters. This reduced the

photometry lists for NGC 1928 and NGC 1939 by ~ 35 per cent, and that for Reticulum by ~ 50 per cent (although for this cluster the removed objects were almost exclusively near the faint limit of detection).

The Reticulum photometry required no further subtraction. For NGC 1928 and 1939, each photometry list was split into three groups according to radius from the centre of the cluster[†]. The aim was to select two radii (r_1 and r_2) for each cluster, so that the de-

[†] We determined the two cluster centres by eye – a procedure accurate enough for present purposes given the very compact nature of both objects.

tections within r_1 defined as clean a cluster sample as possible, while those outside r_2 defined a clean field sample. The sample in between r_1 and r_2 consisted of a mixed field/cluster sample. A small amount of experimentation allowed appropriate values for these radii to be chosen. To define r_1 , photometry lists were assembled for all stars inside $r = 5\text{--}25''$ at $1''$ intervals. CMDs were constructed for each of these lists, and r_1 selected to produce a well defined CMD with as little field contamination as possible. For NGC 1928, $r_1 = 12''$, while for NGC 1939 $r_1 = 15''$. These results are consistent with the fact that NGC 1928 is somewhat more compact than NGC 1939 (see Fig.1), as well as the fact that NGC 1928 is set against a somewhat denser field than NGC 1939 (see Fig. 2) – both of which suggest that r_1 should be smaller for NGC 1928 than NGC 1939. We note that for these measurements and all subsequent calculations, all stars within $12''$ of the centre of NGC 1938 on the NGC 1939 frames were excluded since a large fraction do not belong either to NGC 1939 or its background field. The characteristics of this cluster are described briefly in Section 4.4.

Selecting radius r_2 was a matter of estimating the tidal radius (r_t) for each cluster. Calculating the surface density of stars in radial bins of width $5''$ from $50\text{--}140''$ showed the density to be approximately constant beyond $\sim 90''$ for NGC 1928 and $\sim 100''$ for NGC 1939. These measurements are consistent with previous measurements for other compact LMC bar clusters. For example Olsen et al. (1998) constructed King models for NGC 1754, 1835, 2005, and 2019, and found $r_t \sim 115, 85, 105$, and $145''$ respectively. Similarly, Mateo (1987) measured $r_t \sim 50, 145$, and $160''$ for NGC 1754, 1786, and 1835, respectively. Elson (1985) presented a high quality surface brightness profile and King model for NGC 1835 (the most massive of the old LMC bar clusters, see Mackey & Gilmore (2003a)), and measured $r_t \sim 190''$ formally from the model. However, her profile (her Figure 4a) shows the surface brightness to be greater than 10 mag below the central value even by $r \sim 100''$. Hence, we set $r_2 = 100''$ for NGC 1928 and $r_2 = 110''$ for NGC 1939. While these radii are likely smaller than the true tidal radii for these clusters, they were perfectly adequate for present purposes – allowing field samples of 22 000 and 17 000 stars, respectively. The field star density was found to be 1.48 arcsec^{-2} for NGC 1928, and 1.29 arcsec^{-2} for NGC 1939.

We subjected the photometry samples between r_1 and r_2 to two statistical subtraction procedures. The first involved using the central (cluster) CMD to subtract a matching CMD from the sample, leaving the field stars. The necessary number of subtractions was calculated by using the measured field star density to estimate the expected total number of field stars in the region between r_1 and r_2 . This in turn defined the expected number of cluster stars in the region – that is, the required number of subtractions. We did not account for detection completeness in these estimates. Since regions closer in to the cluster have higher stellar densities, the detection completeness decreases with decreasing radius. The completeness is also a function of stellar magnitude and colour. Because the density of detected field stars in the region between r_1 and r_2 is, overall, less than in the outer region, assuming full completeness in this area leads to an over-estimate of the number of field stars in the intermediate region and hence an under-estimate of the cluster population. However, this was not a significant problem for the present work, primarily because the area suffering from the greatest incompleteness is within r_1 for both clusters. For radii greater than r_1 we estimate the completeness to be greater than 90 per cent for all areas of interest on the CMD (i.e., excluding the lower main sequences, where photometric errors are, in any case, large). In addition, our primary aim was not to obtain a subtraction of *all* possible cluster

stars. Rather, we wanted to observe clean CMDs for NGC 1928 and 1939 for the first time, for the purposes of photometric study. Had we been interested in total number counts (as we would be in the construction of a brightness profile, for example) full artificial star tests would have been carried out (see Mackey & Gilmore, in prep.).

The subtraction process was as follows. First, a random star from the central region CMD was selected. On the intermediate region CMD, all non-subtracted stars within a 3σ error ellipse from this star were located, and one randomly subtracted. If there were no stars within the ellipse, the nearest neighbour was subtracted, providing it did not lie unreasonably distant from the point (i.e., not more than $\sim 6\sigma$). This process was repeated the required number of times to obtain a realization of the subtracted cluster CMD. In any such realization, multiple selections of a central region star were allowed, but a star could not be subtracted from the intermediate region more than once.

For both NGC 1928 and 1939, one hundred CMD realizations were calculated. With these complete, each star in the intermediate region was checked to find how many times it had been subtracted. Stars with a large number of subtractions to their name were most likely to be cluster members. For both clusters, a histogram of this statistic was constructed, allowing a suitable cut-off to be estimated. A small amount of experimentation showed that selecting all stars with more than 75 subtractions provided clean, well-defined CMDs.

The second subtraction method was very similar, but involved using the outer (field) CMD to subtract a matching CMD from the intermediate sample, leaving the cluster stars. The required number of subtractions was again determined using the measured field star density in the outer region. As before, detection completeness was not accounted for, meaning the estimated number of field stars (and hence subtractions) was over-estimated. The subtraction process was identical, except this time random stars from the outer region CMD were selected. Once again, one hundred realizations of each cluster's CMD were obtained and the stars appearing the most times in these CMDs selected as the most likely cluster members. For this method, selecting all stars with more than 50 subtractions provided good CMDs. Because of the differential reddening present in the outer field regions of the NGC 1939 frame, this subtraction method was not as effective for this cluster. Nonetheless, adequate results were obtained.

3.2 Final Cluster CMDs

The final cleaned, field-subtracted CMDs for NGC 1928, 1939, and Reticulum appear in Fig. 3. In this Figure, the CMDs for NGC 1928 and 1939 represent the combined results of the two subtraction processes. Stars within r_1 have also been plotted for both clusters, since these are very predominantly cluster members. To the best of our knowledge these are the first published CMDs for NGC 1928 and 1939. It can clearly be seen that these two clusters are very old, thus confirming the results obtained by Dutra et al. (1999) using integrated spectroscopy. Both clusters appear to possess well populated horizontal branches, consisting almost entirely of blue stars. In this respect they strongly resemble the old LMC clusters Hodge 11 (Walker 1993; Mighell et al. 1996; Johnson et al. 1999) and NGC 2005 (Olsen et al. 1998). In addition, NGC 1928 apparently possesses an extended blue HB, falling to $V \sim 23$. The effects of differential reddening on the field subtraction for NGC 1939 can be seen in its lower main sequence, which exhibits a sharp cut-off

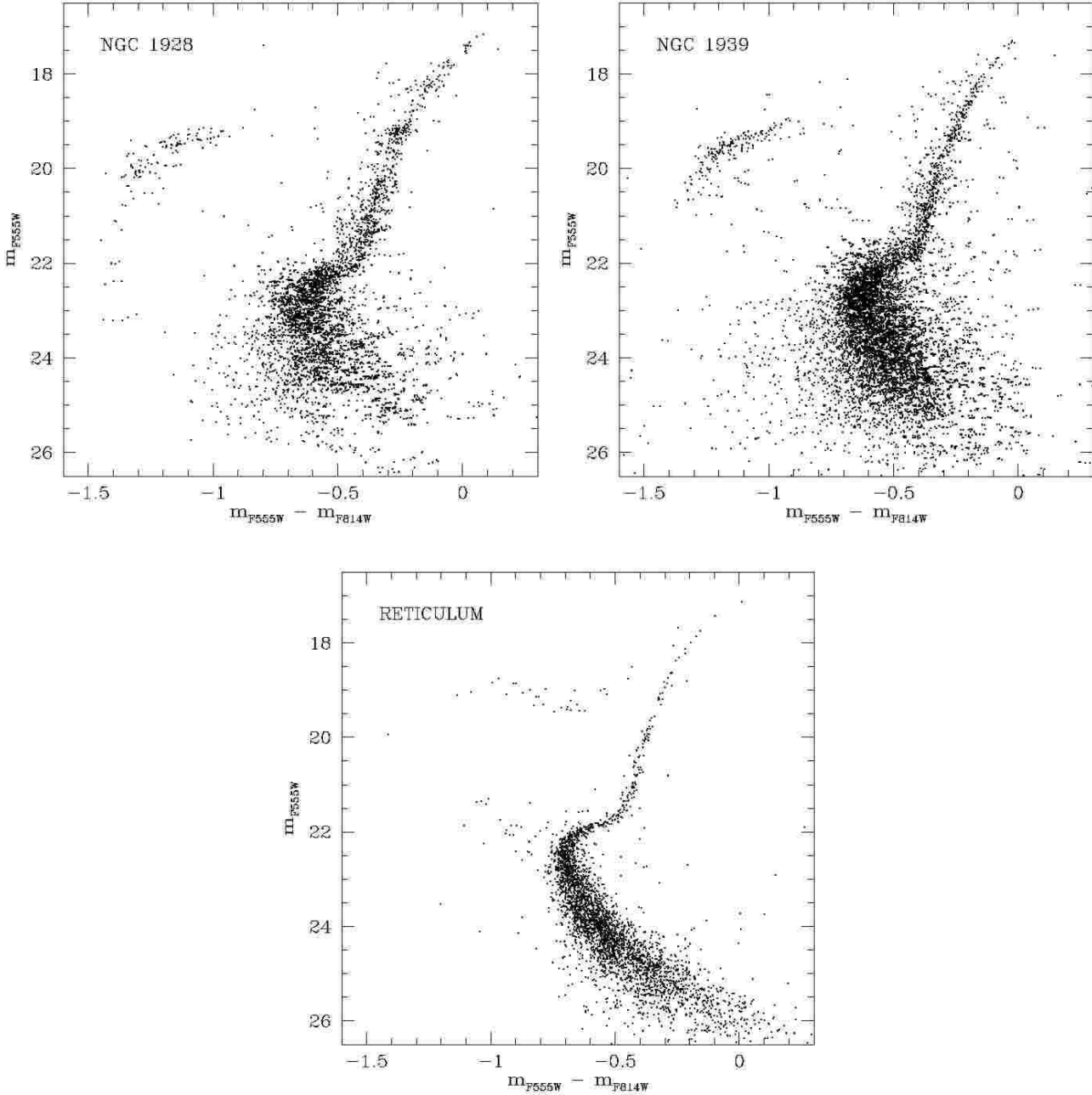


Figure 3. Cleaned, field-subtracted colour-magnitude diagrams for the three clusters. For both NGC 1928 and 1939, the plotted points are the combined results of the two field subtraction algorithms, along with the central sample of stars.

to the red. The remainder of the CMD has not been significantly affected by this problem.

Reticulum is also seen to be an old cluster, with a horizontal branch primarily consisting of stars within and to the red of the instability strip. A significant population of blue stragglers also appears to be present. This CMD confirms the earlier results of Walker (1992); Johnson et al. (2002); Marconi et al. (2002); and Monelli et al. (2003).

Ideally, we would like to use the final CMDs to provide photometric measurements of the cluster reddenings and metallicities, and to place some constraints on their ages. However, such calculations generally require the photometry to be on a standard mag-

nitude scale – in this case, Johnson-*V* and Cousins-*I*. At the time of writing, no transformations from the ACS/WFC STmag system to the Johnson-Cousins *VI* system are yet available. Nonetheless, we were able to determine an approximate transformation. One of the clusters from the present study – Reticulum – has previously been observed with *HST*/WFPC2 through the F555W and F814W filters (as part of program 5897). Calibrations for these filters to the Johnson-Cousins *VI* system *do* exist and are well established (Holtzman et al. 1995; Dolphin 2000b). The relevant archived data-groups are labelled u2xj0605b ($5 \times$ F555W frames – two with exposure durations of 260 s and three with exposure durations of 1000 s) and u2xj0608b ($6 \times$ F814W frames – two with exposure

durations of 260 s and four with exposure durations of 1000 s). Unfortunately, these observations did not image the cluster core, but rather are centred approximately $1.5'$ to the north west. Fig. 4 shows the positions of the two observation sets overlaid on a DSS image of Reticulum. While there is a small overlap, the number of common stars was not large enough to derive a point-by-point photometric transformation. Nonetheless, it was still possible to calculate a global transformation.

First, photometric measurements were performed on the archival WFPC2 images using HSTPHOT (Dolphin 2000a). The measurement procedure is described fully by Mackey (2004), and is identical to the procedure used by Mackey & Gilmore (2003d) to measure RR Lyrae stars in the globular clusters of the Fornax dwarf galaxy. The resultant CMD may be seen in Fig. 5.

We next determined fiducials for both the CMD from the present study (in the ACS/WFC STmag system) and the CMD from the archival WFPC2 data (in V , $V - I$). The main sequences are well populated enough that the fiducials below the turn off could be calculated by forming magnitude bins and finding the mode in colour for each. This would typically also work for the RGB, but on neither CMD is this region particularly well populated (Reticulum is a very sparse cluster). Thus, the RGB fiducials were determined by eye, as were the fiducials around the turn-off and sub-giant branch (SGB). These latter could not be measured via a simple binning technique because they are neither horizontal nor vertical. As can be seen in Figs. 3 and 5, the dispersion in these regions of each CMD is small (particularly for the ACS measurements), so the by-eye procedure should not introduce any large errors. This algorithm is very similar to many used in previous studies (see e.g., Johnson et al. (1999)). The horizontal branch (HB) levels were determined using the (very few) stars just to the blue of the instability strip. Due to the lack of multi-epoch observations (especially for the ACS data), the RR Lyrae regions possess a significant spread in magnitude due to the intrinsic stellar variability.

On each CMD, the colour of the main sequence turn-off (MSTO) was determined by fitting a second-order polynomial to the data in this region, and finding the bluest point of the fit. The magnitude of a main-sequence (MS) reference point $V_{0.05}$ (the point on the MS which is 0.05 mag redder than the MSTO) was then determined by interpolating along the fiducial line. These two values are traditionally used to register cluster CMDs for the purposes of differential age comparison (VandenBerg et al. 1990) (see Section 4.3); however our purpose here was to determine a linear shift between the ACS/WFC photometry, and the standard Johnson-Cousins scale. By moving the ACS/WFC fiducial so that the colour of its MSTO matched that for the WFPC2 fiducial, and its $V_{0.05}$ matched that for the WFPC2 fiducial, this transformation was calculated. We found that $V - m_{F555W} = 0.03$ and $(V - I) - (m_{F555W} - m_{F814W}) = 1.31$. The registered fiducials may be seen in the top panel of Fig. 5, while the shifted ACS fiducial is plotted on the WFPC2 CMD in the lower panel of this Figure. The registration is very close across all parts of both fiducials, except in the RGBs, which are separated slightly. The upper portion of the WFPC2 RGB is somewhat uncertain due to a lack of stars; however the separation persists into the lower RGB area, which is well defined for both sets of photometry. The HB levels, on the other hand, match closely. Our derived transformation implies that $I - m_{F814W} = -1.28$, which matches perfectly the result of Brown et al. (2003), who found exactly this relation for a 5000 K stellar spectrum.

While it is almost certain that the true transformation is not linear (the WFPC2 transformations are parametrized by quadratic

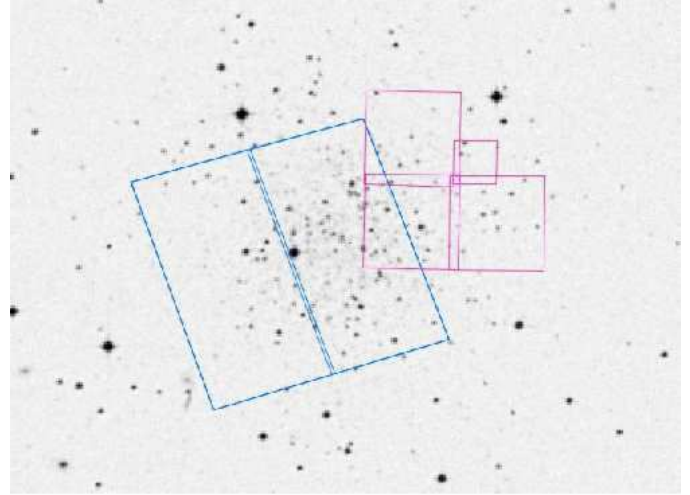


Figure 4. Position and orientation of the present ACS observations of Reticulum and the archival WFPC2 observations, superimposed on a DSS image. North is toward the top and east to the left. For some idea of the scale, the ACS FOV is approximately $202''$ on a side. There is a small overlap between the two sets of observations, but the bulk of the WFPC2 field lies more than an arcminute to the north-west of the ACS frames.

functions – see Holtzman et al. (1995)), it is clear from the good match between the two Reticulum fiducials that the present approximation is a good one, and certainly accurate enough for our purposes. It is not clear why the two RGBs show a small offset (~ 0.02 mag). It is possible that this is a second order distortion (e.g., a stretch along the colour axis). If this were the case, we would expect a similar offset between the lower main sequences, which lie at approximately the same colour as the RGBs. There is indeed a hint of such an offset between the two sequences on the lower MS, although it is noted that the photometric errors are large at these faint magnitudes. We would also expect the discrepancy to become larger with redder colours, and again, while there is a hint of this on the RGBs, the upper two points on the WFPC2 fiducial are quite uncertain. Nonetheless, the possibility of second-order distortions (of the order of 0.02 mag) must be considered in any calculations involving the ACS/WFC CMDs, such as those in the next Section, until the full ACS/WFC calibration is complete and comprehensive transformation equations are published.

4 CLUSTER PROPERTIES

4.1 Abundances and Reddenings

We employed the technique of Sarajedini (1994) to calculate photometric estimates for the reddening and metallicity of each of the three clusters. In this technique, the height of the RGB above the HB at intrinsic (dereddened) colour $(V - I)_0 = 1.2$ is used to determine the metallicity (this parameter is labelled $\Delta V_{1.2}$), while the reddening is obtained from the colour of the RGB at the level of the HB, $(V - I)_g$. The input parameters are hence the V magnitude of the HB and some parametrization of the shape of the RGB – we chose to use the common procedure of fitting a second order polynomial to the RGB points above the HB. This took the form $(V - I) = a_0 + a_1 V + a_2 V^2$. We fit this relation iteratively, discarding outlying points on each iteration. The results may be seen in Table 2, and graphically in Fig. 6.

Measuring accurately the level of the HB (V_{HB}) was not a

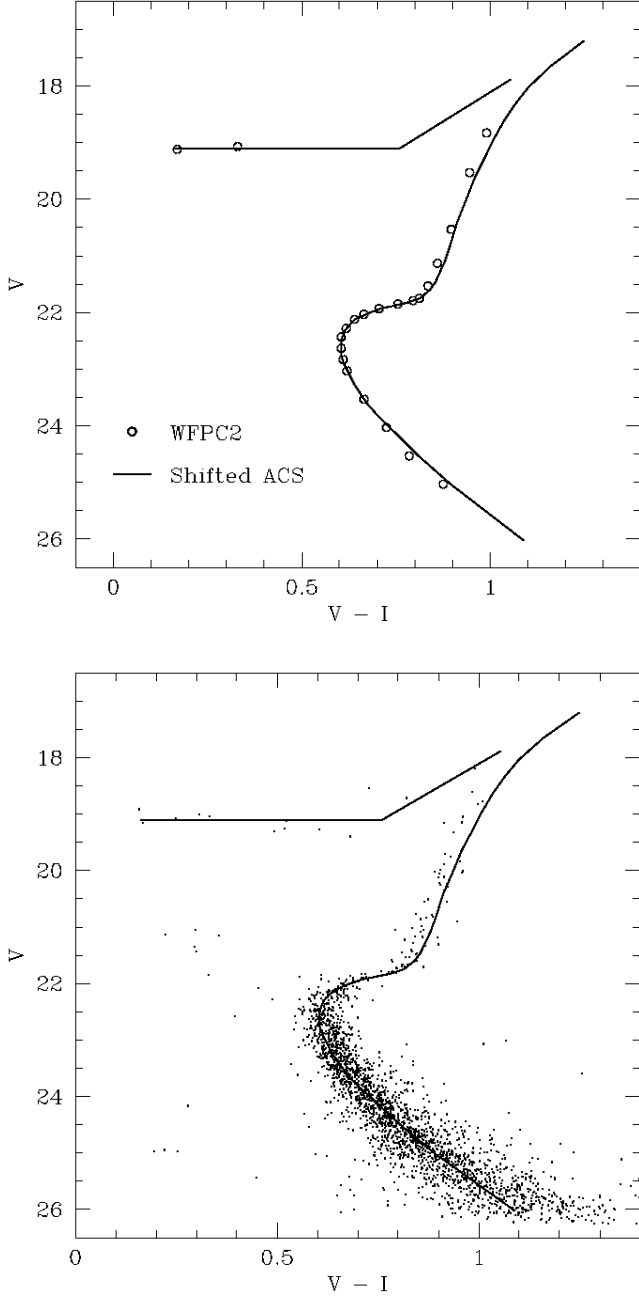


Figure 5. The shifted Reticulum fiducial as determined from ACS/WFC photometry, compared with the Reticulum fiducial from the WFPC2 photometry (upper panel) and the WFPC2 photometry itself (lower panel). The ACS/WFC fiducial has been moved 0.03 mag fainter in V and 1.31 mag redder in colour, as described in the text.

trivial procedure, especially for NGC 1928 and NGC 1939, which have predominantly blue HB morphologies, and unknown reddenings. Ideally in such cases, we would like to use the level of the reddest HB stars on the blue side of the instability strip. Using the RR Lyrae stars in four globular clusters in the Fornax dwarf spheroidal galaxy, Mackey & Gilmore (2003d) found the blue edge of the instability strip to lie at an intrinsic colour of $(V - I)_{\text{BE}} = 0.28 \pm 0.02$. We employed an iterative technique to determine V_{HB} in conjunction with $E(V - I)$ and $[\text{Fe}/\text{H}]$ for

each cluster. We first determined estimates for V_{HB} using the reddest end of the populated blue HB region for NGC 1928 and 1939, and the bluest HB stars for Reticulum. For a given cluster, we then solved for $E(V - I)$ and $[\text{Fe}/\text{H}]$ following Sarajedini (1994), and used the value of $E(V - I)$ so determined to locate the HB stars just to the blue of the edge of the instability strip at $(V - I)_0 = 0.28$. These stars defined a new value for V_{HB} , and the process was iterated until convergence. We estimated the (random) errors in these values again using the prescription of Sarajedini (1994). The accuracy with which we could measure V_{HB} was generally ± 0.05 mag, while that for $(V - I)_g$ was greater – because of the narrowness of the RGB sequences and the stability of the quadratic fits – at ± 0.01 mag. Ten thousand new fits per cluster were calculated, each time using a value of V_{HB} chosen randomly from a distribution with $\sigma = 0.05$ about the genuine measurement of V_{HB} , and a new value of $(V - I)_g$ selected randomly from a distribution with $\sigma = 0.01$ about the genuine measurement of $(V - I)_g$. The standard deviations in the new sets of $E(V - I)$ and $[\text{Fe}/\text{H}]$ defined the random errors in these quantities.

The final reddening and metallicity values are recorded in Table 2 along with the estimated errors. NGC 1939 is a metal-poor cluster ($[\text{Fe}/\text{H}] = -2.10$), while Reticulum is somewhat more metal-rich ($[\text{Fe}/\text{H}] = -1.66$). In contrast, NGC 1928 is significantly more metal-rich again with $[\text{Fe}/\text{H}] = -1.27$ – rendering it the most metal-rich of the known old LMC bar clusters. Examination of the clean CMD for NGC 1928 supports this result, as there is a clear RGB luminosity function bump at approximately V_{HB} . Such a bump is characteristic of clusters with intermediate metal abundance (see e.g., Sarajedini & Forrester (1995)).

Our new results are all consistent with previous measurements and estimates, where these are available. NGC 1928 and 1939 have been poorly studied, with each possessing only one previous metallicity estimate. These are from Dutra et al. (1999) who compared their integrated spectra of NGC 1928 and 1939 to those for three Galactic globular clusters to estimate that $[\text{Fe}/\text{H}] \approx -1.2$ for NGC 1928, and $[\text{Fe}/\text{H}] \approx -2.0$ for NGC 1939. According to Burstein & Heiles (1982), the foreground reddening in the direction of both is $E(B - V) = 0.09$, which corresponds to $E(V - I) \approx 0.12$ (see e.g., Mackey & Gilmore (2003c)). Reticulum has been more extensively studied. Walker (1992) found that $[\text{Fe}/\text{H}] = -1.7 \pm 0.1$ by studying the RR Lyrae stars in the cluster, while Suntzeff et al. (1992) obtained a spectroscopic measurement of $[\text{Fe}/\text{H}] = -1.71 \pm 0.1$. Both of these measurements are in excellent agreement with our photometric determination that $[\text{Fe}/\text{H}] = -1.66 \pm 0.12$. On the reddening front, we measured $E(V - I) = 0.07 \pm 0.02$. Walker (1992) found that $E(B - V) = 0.03 \pm 0.02$ (i.e., $E(V - I) = 0.04 \pm 0.03$) but notes that the colours of his RR Lyrae sample at minimum light could imply a slightly higher reddening: $E(B - V) = 0.05 \pm 0.02$ (i.e., $E(V - I) = 0.07 \pm 0.03$). Marconi et al. (2002) suggest that the reddening towards Reticulum could be twice as large as that suggested in the literature (i.e., $E(V - I) \sim 0.08$). All of these estimates are in good agreement with our new measurement.

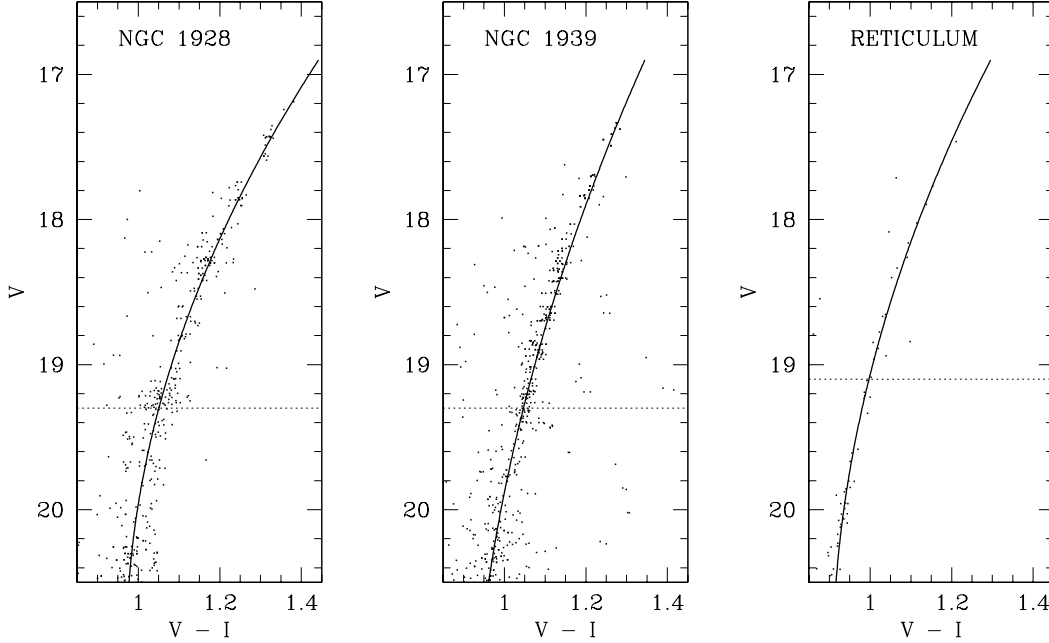
As a final consistency check, if we adopt the calibration between intrinsic RR Lyrae brightness and metallicity of Chaboyer (1999):

$$M_V(\text{RR}) = 0.23([\text{Fe}/\text{H}] + 1.6) + 0.56, \quad (4)$$

we can calculate distance moduli (μ) for the three clusters. We find that, with $A_V = 2.37E(V - I)$ (e.g., Mackey & Gilmore (2003c)), $\mu = 18.47 \pm 0.12$ for NGC 1928 and $\mu = 18.48 \pm 0.16$ for NGC 1939, where the errors represent only the effect of random measure-

Table 2. Results of the simultaneous determination of cluster reddenings and metallicities.

Cluster	V_{HB}	a_0	a_1	a_2	$\Delta V_{1.2}$	[Fe/H]	$E(V - I)$
NGC 1928	19.30 ± 0.05	13.45040	-1.18991	0.02836	1.64 ± 0.15	-1.27 ± 0.14	0.08 ± 0.02
NGC 1939	19.30 ± 0.05	8.22729	-0.65527	0.01468	2.52 ± 0.20	-2.10 ± 0.19	0.16 ± 0.03
Reticulum	19.10 ± 0.05	10.56360	-0.91361	0.02161	2.05 ± 0.13	-1.66 ± 0.12	0.07 ± 0.02

**Figure 6.** Quadratic fits to the three cluster RGBs, used for the reddening and metallicity determinations. The dotted lines indicate the measured HB levels.

ment errors from V_{HB} , $E(V - I)$ and [Fe/H]. For Reticulum we find $\mu = 18.39 \pm 0.12$. All these estimates are in good agreement with the canonical distance to the LMC: $\mu_{\text{LMC}} \approx 18.50$.

Given the uncertainties in the (approximate) photometric transformations detailed in Section 3.2, it is important to discuss briefly the potential effect of these on our metallicity and reddening measurements. The metallicity determination is obtained from a purely differential process (Eq. 4 in Sarajedini (1994) shows [Fe/H] to be dependent only on $\Delta V_{1.2}$) and is thus affected only by any second or higher order distortion over the range $\Delta V_{1.2}$ in V and $1.2 - (V - I)_g$ in $V - I$. Since both of these, especially the latter, are relatively small values, these distortions are unlikely to be large, and we estimate the systematic error so introduced to be less than 0.05 dex. Since the distortion apparently produces an RGB which is slightly redder than appropriate (see Fig. 5), the bias is towards measurements which are too metal-rich. The reddening estimates are dependent on both $(V - I)_g$ and [Fe/H] (Sarajedini Eq. 3). The dependence on [Fe/H] is weak, so the primary error is introduced through $(V - I)_g$, which could be ~ 0.02 mag too red (see Section 3.2). This would be transferred directly to the $E(V - I)$ estimate, so it is possible these are too high by ~ 0.02 . Nonetheless, the consistency of our estimates with both literature measurements and the LMC distance scale lead us to have confidence in the accuracy and validity of our results.

4.2 Horizontal Branch Morphologies

Although we have images at only one epoch, and therefore no stellar variability information, it is possible to calculate a quantitative measure of each cluster's HB morphology now that accurate reddening values are known. As part of their study of 197 RR Lyrae stars in four globular clusters belonging to the Fornax dwarf galaxy, Mackey & Gilmore (2003c) provided accurate measurements of the intrinsic $V - I$ colours of the red and blue edges of the instability strip at the level of the horizontal branch. They found $(V - I)_{\text{BE}} = 0.28 \pm 0.02$ and $(V - I)_{\text{RE}} = 0.59 \pm 0.02$. These values can be used to count the number of blue HB stars, red HB stars, and stars on the instability strip. The HB morphology is usually parametrized by the index $(B - R)/(B + V + R)$ of Lee, Demarque & Zinn (1994), where B is the number of BHB stars, V the number of variable HB stars, and R the number of RHB stars. Because we have only single epoch observations it is possible that some variables might lie outside the adopted instability strip edges (although this will not affect the morphology indices significantly, especially for NGC 1928 and 1939). In addition, because of the difficult field star subtractions necessary for NGC 1928 and NGC 1939, our number counts are commensurately uncertain. It is nonetheless worthwhile to make an attempt to calculate the HB morphology for these clusters since no previous estimates exist.

For NGC 1928 we counted $R = 2_{-2}^{+1}$, $V = 3_{-3}^{+1}$, and $B =$

Table 3. Results of the CMD registration and relative age dating measurements (vertical technique).

Cluster	$(V - I)_{\text{TO}}$	V_{TO}	$(V - I)_{0.05}$	$V_{0.05}$	V_{HB}	$\Delta V_{\text{TO}}^{\text{HB}}$	$\Delta V_{0.05}^{\text{HB}}$
NGC 1928	0.674	22.851	0.724	23.85	19.30	3.55	4.55
NGC 1939	0.660	22.910	0.710	23.69	19.30	3.61	4.39
Reticulum	0.603	22.627	0.653	23.41	19.10	3.53	4.31
M92	0.558	18.712	0.608	19.49	15.18	3.53	4.31
M3	0.595	19.173	0.645	19.98	15.75	3.42	4.23
M5	0.629	18.590	0.679	19.44	15.18	3.41	4.26
NGC 1466	0.622	22.860	0.672	23.73	19.32	3.54	4.41
NGC 2257	0.612	22.530	0.662	23.40	19.10	3.43	4.30
Hodge 11	0.628	22.812	0.678	23.58	19.11	3.70	4.47

Table 4. Results of the relative age dating measurements (horizontal technique).

Cluster Name	[Fe/H]	$\delta_{2.5}$	Reference Cluster	[Fe/H]	$\delta_{2.5}$	$\delta(V - I)$	$\Delta\tau$ (Gyr)
NGC 1928	-1.27	0.285	M5	-1.27	0.281	0.003	-0.2
NGC 1939	-2.10	0.293	M92	-2.28	0.283	0.013	-1.3
			NGC 1466	-2.17	0.289	0.006	-0.5
				(-1.85)			(+0.6)
			Hodge 11	-2.06	0.276	0.021	-0.9
Reticulum	-1.66	0.309	M3	-1.54	0.275	0.038	-1.4
			NGC 2257	-1.63	0.290	0.023	-1.0
				(-1.85)			(-1.8)

111^{+13}_{-11} , including the putative extended BHB (~ 11 stars). For the more heavily populated NGC 1939 HB we counted $R = 3 \pm 3$, $V = 5^{+1}_{-5}$, and $B = 173^{+10}_{-12}$. These star counts result in a HB index of $(B - R)/(B + V + R) = 0.94^{+0.06}_{-0.04}$ for both clusters, confirming their status as having almost exclusively blue HB morphologies. Reticulum clearly has a more evenly spread HB, and we count $R = 5^{+2}_{-4}$, $V = 18 \pm 3$, and $B = 5^{+0}_{-2}$, meaning a HB index of 0.00 ± 0.15 . This is entirely consistent with the result of Walker (1992) who measured an index of $-0.04^{+0.00}_{-0.05}$.

4.3 Ages

While it is quite evident from the CMDs presented in Fig. 3 that the three clusters from the present study exhibit all the photometric qualities of the oldest globular clusters, it is useful to obtain some quantitative measure of their ages. The best way to achieve this for the current sample is via differential comparison with clusters which have well established ages. To this end, we employed cluster fiducials for the Galactic globular clusters M92, M3, and M5 measured by Johnson & Bolte (1998), and for the LMC globular clusters NGC 1466, NGC 2257, and Hodge 11 measured by Johnson et al. (1999).

There is a large number of procedures available in the literature for the relative age dating of globular clusters. Perhaps the two most widely used techniques are the so-called vertical and horizontal methods. The vertical method relies on the fact that the difference between the magnitude of the MSTO and the HB is age dependent, with older clusters generally having larger values of this parameter. Similarly, the horizontal method relies on the fact that the length of the SGB is shorter for older clusters, which thus have bluer RGBs. Both techniques have a metallicity dependence

which must be accounted for. Metallicities for the present LMC clusters and the six reference clusters are listed in Table 4. For M92, M3, and M5 these have been obtained from the database of Harris (1996), while for NGC 1466, 2257, and Hodge 11 they are taken from various literature sources. Olszewski et al. measured spectroscopic abundances for NGC 1466 and Hodge 11 ($[\text{Fe}/\text{H}] = -2.17$ and -2.06 , respectively); however Johnson et al. (1999) suggest a slightly more metal rich value for NGC 1466 ($[\text{Fe}/\text{H}] = -1.85$). Johnson et al. also suggest $[\text{Fe}/\text{H}] = -1.85$ is appropriate for NGC 2257 based on several previous estimates; however Dirsch et al. (2000) obtained $[\text{Fe}/\text{H}] = -1.63$ based on a photometric study.

For NGC 1928, NGC 1939, and Reticulum, we determined the colour and magnitude of the MSTO together with the MS reference point 0.05 mag redder than the MSTO using exactly the same technique as that described in Section 3.2. The results may be found in Table 3. These points were used for two purposes – measuring the vertical method age indicators, and registering CMDs for the horizontal method (again, as described in Section 3.2). For the reference clusters, we lacked the full photometry sets, so could not apply exactly the same procedure. However, we found it perfectly adequate to fit a quadratic function to the fiducial points around the MSTO for these clusters. Johnson et al. (1999) provide measurements of $(V - I)_{\text{TO}}$ and $V_{0.05}$ for NGC 1466, 2257, Hodge 11, M92, and M3. We find our calculations (again, see Table 3) to match their results very closely, which leads us to have confidence in our procedure and our measurements for M5. We estimate that our determinations of V_{TO} and $V_{0.05}$ are accurate to ± 0.05 mag, while those for $(V - I)_{\text{TO}}$ and $(V - I)_{0.05}$ are accurate to better than ± 0.01 mag.

Our measured values for $\Delta V_{\text{TO}}^{\text{HB}}$, the difference in V between

the level of the HB and the MSTO are listed in Table 3. Both of these levels are quite uncertain – the HB because of some intrinsic width, as well as scatter due to stellar variability for Reticulum, and the significant weighting to the blue for NGC 1928 and 1939; and the MSTO because the MS is vertical in the turn-off region. We estimate our measurement errors in $\Delta V_{\text{TO}}^{\text{HB}}$ to be approximately ± 0.1 mag. The results in Table 3 show only a small dispersion among the clusters, even ignoring metallicity effects. Rosenberg et al. (1999) used two sets of theoretically calculated isochrones to provide a calibration for age as a function of $\Delta V_{\text{TO}}^{\text{HB}}$ and metallicity. This appears in their Figure 3, which shows the significant majority of the 34 Galactic globular clusters in their sample to lie within a narrow band of ~ 2 Gyr width about mean values of 14.3 Gyr and 14.9 Gyr for the two isochrone sets. Placing our clusters on this diagram (using the metallicities listed in Table 4) shows NGC 1928 and Reticulum to lie within this band, along with all the reference clusters except Hodge 11. This cluster, along with NGC 1939 fall ~ 2 Gyr older than the upper limit of the Rosenberg et al. 2 Gyr band.

In order to combat the uncertainty in $\Delta V_{\text{TO}}^{\text{HB}}$ introduced by measuring V_{TO} , Buonanno et al. (1998) introduced a calibration for a similar vertical parameter, $\Delta V_{0.05}^{\text{HB}}$ – the difference in V between the level of the HB and $V_{0.05}$. Because the MS is sloped at $V_{0.05}$, this measurement is in theory more accurate (although formally, our errors are the same). We therefore calculated $\Delta V_{0.05}^{\text{HB}}$ for each cluster for comparison with the Buonanno et al. calibration. These measurements are also listed in Table 3. The relevant calibration appears in Figure 7(a)-(c) of Buonanno et al., for three isochrone sets. We note that this calibration is based on $(V, B - V)$ CMDs, however it should provide some indication of age homogeneity or otherwise in our cluster sample. Plotting the clusters on this Figure again shows them to lie within a band of width ~ 2 Gyr, along with 14 Galactic globular clusters from the Buonanno et al. sample. The one outlier in our sample is NGC 1928, which lies ~ 2 Gyr older than the band. For the three isochrone sets, the best fitting mean ages are 14 Gyr, 12 Gyr and 15 Gyr, respectively.

Rosenberg et al. (1999) provide a calibration for a horizontal dating method in addition to their vertical method calibration. The relevant parameter in this case is $\delta_{2.5}$, the difference in $V - I$ between the MSTO and a point on the RGB 2.5 mag brighter than the MSTO. Our measurements of this parameter for all the clusters are listed in Table 4. Again, these results show a good deal of internal consistency, suggesting small relative age differences. This is confirmed by consideration of Figure 4 in Rosenberg et al. which shows their age calibration including metallicity effects, again for two isochrone sets. As for the vertical age indicator, the $\delta_{2.5}$ values place all the present LMC and reference clusters within the same 2 Gyr-wide band. On this occasion, there are no significant outliers.

Finally, we obtained a more quantitative measure of the relative cluster ages using the horizontal method calibration of Johnson et al. (1999). For this process, we first registered two cluster CMDs using $(V - I)_{\text{TO}}$ and $V_{0.05}$, and then calculated the mean difference in colour between their RGBs from the base to the HB, $\delta(V - I)$. This was achieved using the procedure of Johnson et al. (1999). A straight line was fit to the RGB section for the reference cluster, and then the weighted average of the difference in colour between this line and the RGB stars for relevant the LMC cluster. Since $\delta(V - I)$ is sensitive to both age and metallicity, it was important to choose a reference cluster with similar metallicity to the LMC cluster under consideration. With the available clusters we had the following six matches: NGC 1928 and M5; NGC 1939 and M92, NGC 1466, and Hodge 11; Reticulum and M3, and NGC 2257. The results of the

$\delta(V - I)$ calculations are listed in Table 4, while Fig. 7 shows the reference cluster fiducials registered to the relevant LMC cluster fiducials. It is immediately clear from these plots that there cannot be a large age difference between the present three clusters and the oldest Galactic and LMC globular clusters. In order to quantify this, we use the results of Johnson et al. (1999) who provide relations between $\delta(V - I)$, age and metallicity using two theoretical isochrone sets. The differences in the two calibrations are not large and we adopt a mean relation. First we correct $\delta(V - I)$ between an LMC cluster and a reference cluster for metallicity effects using

$$\delta(V - I) = -0.0745(\Delta[\text{Fe}/\text{H}]) \quad (5)$$

and then estimate the age difference using

$$\delta(V - I) = -0.0205(\Delta\tau) \quad (6)$$

where τ represents age in Gyr. Strictly speaking this calibration is only valid over the metallicity range $-2.26 < [\text{Fe}/\text{H}] < -1.66$; however it is unlikely that extrapolating slightly to $[\text{Fe}/\text{H}] \sim -1.3$ for NGC 1928 and M5 will introduce a large error. The results of the calculations are listed in Table 4. The two reference clusters NGC 1466 and 2257 have differing metallicities listed in the literature, as discussed earlier. Hence, these two clusters have a relative age range, as listed in Table 4.

None of the present three LMC clusters is more than ~ 1.5 Gyr younger than any reference cluster. This offers quantitative evidence that NGC 1928, 1939, and Reticulum are true members of the oldest population of LMC star clusters, and are coeval with the oldest Galactic globular clusters. Supporting evidence is provided by the more qualitative measures offered by the vertical dating technique – the results of which are fully consistent with all the clusters being coeval to within ± 1 Gyr or so. We note that it is possible that our approximate transformation to Johnson V and Cousins I photometry has introduced some systematic error into the relative age measurements – after all, we noted earlier that the transformed RGBs are possibly too red by ~ 0.02 mag. In this context, it is interesting to note that all the $\delta(V - I)$ values are positive, indicating LMC cluster RGBs lying to the red of the reference cluster RGBs. This potential systematic error does not affect our conclusion however, because redder RGBs indicate more youthful clusters. Thus, the $\Delta\tau$ values listed in Table 4 represent the maximum age differences implied by the $\delta(V - I)$ dating technique if the transformation is imperfect in the manner suspected – in reality it is likely that the clusters are even closer in age.

4.4 NGC 1938

It is worth plotting the CMD for the stars within $12''$ of the centre of NGC 1938 – which were removed from the calculations for NGC 1939 (see Section 3.1) – because we could not find any previously published CMDs for this cluster. Fig. 8 shows a close-up of the ACS/WFC F555W observation in the vicinity of NGC 1938 and 1939, with the extraction radius shown. The resultant CMD for NGC 1938 is plotted in Fig. 9. No attempt has been made to remove the field star contamination or the contamination from NGC 1939, the giant branch of which is visible. Nonetheless, a narrow main sequence is clearly evident in this CMD. It is not immediately obvious that this should be associated with NGC 1938 since it is clear from Fig. 2 that it lies in the vicinity of the “young” main sequence of the field population. To investigate this we calculated a crude fiducial for the sequence in Fig. 9 above $m_{\text{F555W}} = 22$. We then counted all the stars less than 0.15 mag perpendicular distance from this fiducial in two bins – an upper bin ($17 \leq m_{\text{F555W}} \leq 20$) and

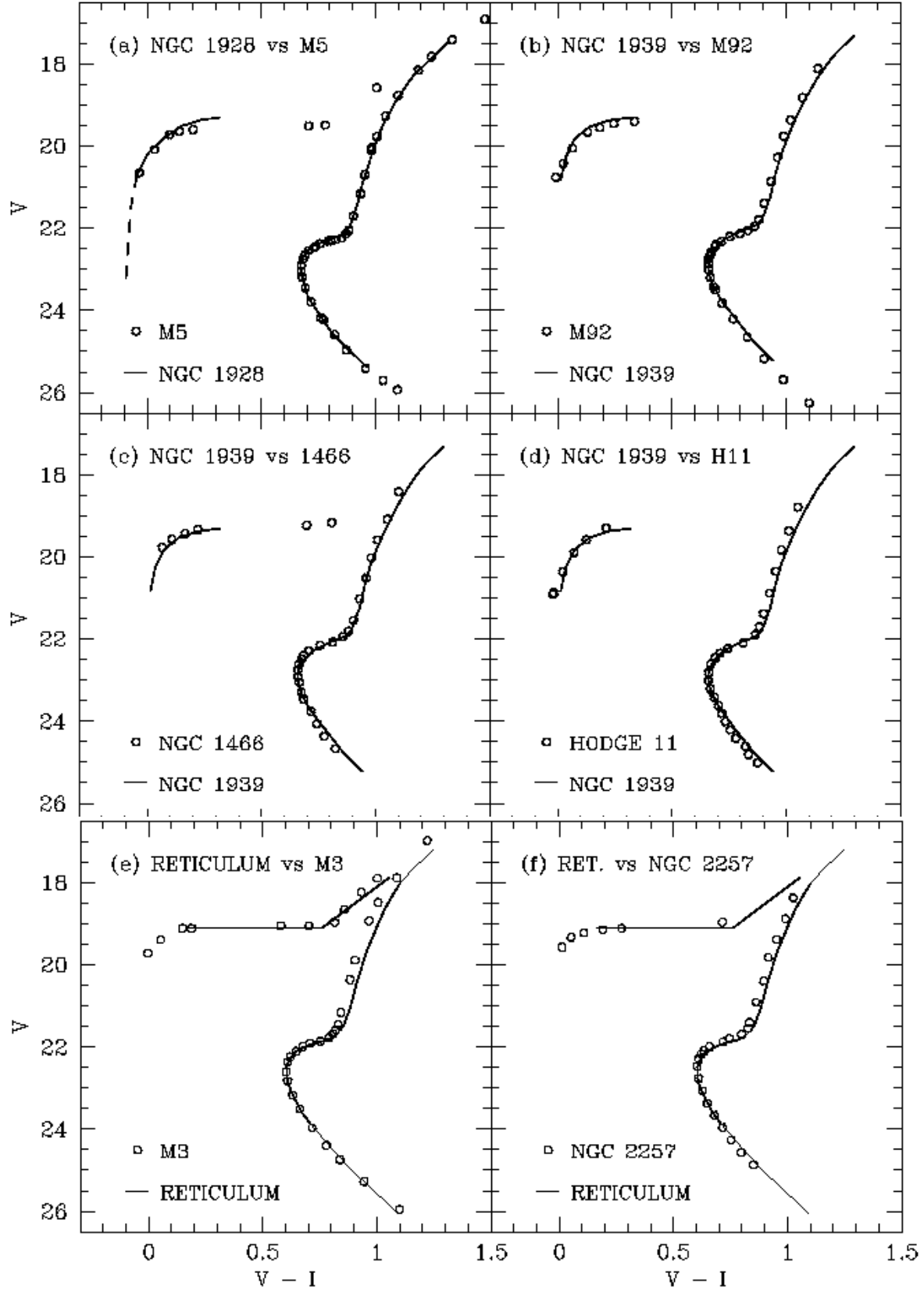


Figure 7. Reference cluster fiducials (open circles) registered to the fiducials for NGC 1928, 1939, and Reticulum (solid lines) using $(V-I)_{TO}$ and $V_{0.05}$.

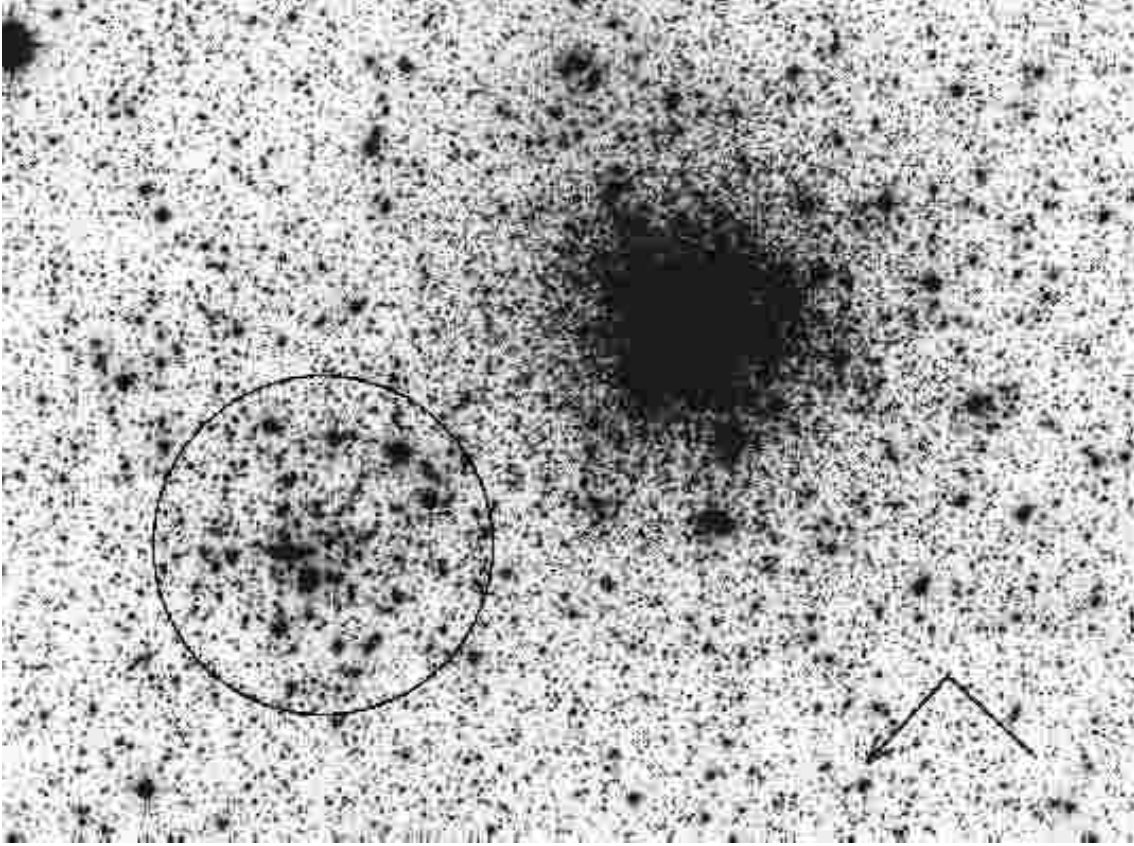


Figure 8. ACS/WFC F555W image of the region surrounding NGC 1939 and NGC 1938 (circled). North and east are indicated (north is in the direction of the arrow). The NGC 1938 extraction radius is $\sim 12''$.

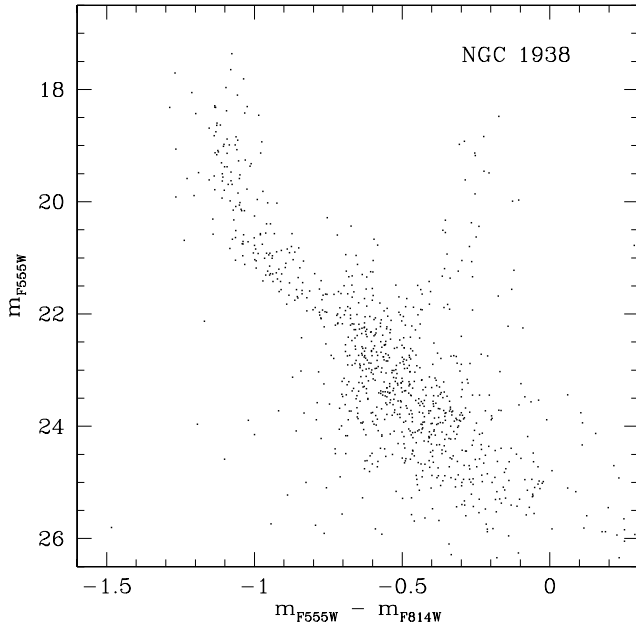


Figure 9. CMD for all stars within the $12''$ extraction radius around NGC 1938. As previously, measurements are in the ACS/WFC STmag system.

a lower bin ($20 \leq m_{F555W} \leq 22$). Next, two field extractions of equivalent area to the NGC 1938 extraction (i.e., with radius $12''$) were made away from both NGC 1938 and 1939 – one at $40''$ to the north-west of NGC 1938, and one $1'$ to the north-east of NGC 1938. These were far enough away not to be contaminated by NGC 1938 or NGC 1939, and close enough not to be affected by serious differential reddening. We then repeated our star counts in these two extractions. In the on-cluster extraction we counted 64 stars in our upper bin and 107 in our lower bin. For the two off-cluster extractions we counted 5 and 8 stars respectively for the upper bin, and 31 and 33 stars respectively for the lower bin. The star counts are clearly significantly enhanced for the on-cluster field, especially for the upper main sequence region. This allows us to confidently associate the sequence observed in Fig. 9 with NGC 1938 and not the general field population.

No turn-off is observed on this sequence to $m_{F555W} \approx V \approx 18$. We use this fact to place an upper limit on the age of NGC 1938. Kerber et al. (2002) provide a CMD for the rich LMC cluster NGC 1831 from WFPC2 observations, which shows the turn-off to be just below $V \approx 18$. Their age estimate for this cluster is $\tau \approx 500$ Myr. Elson & Fall (1988) provide an age calibration for a large number of LMC clusters. Their age estimate for NGC 1831, corrected to a distance modulus of 18.5 is ~ 300 Myr. Together these age estimates provide us with an approximate upper limit for the age of NGC 1938 of ~ 400 Myr. This result is perfectly consistent with the integrated UBV photometry of Bica et al. (1996), which places NGC 1938 in SWB class IVA (where the SWB class refers to the classification of Searle, Wilkinson & Bagnuolo (1980)). This

class brackets the age range 200–400 Myr. Because of the very large age difference between NGC 1938 and 1939, it seems unlikely that these two clusters are physically related – rather, their apparent close proximity is merely a projection effect.

5 SUMMARY

We have used ACS/WFC snapshot observations to obtain colour-magnitude diagrams for the LMC clusters NGC 1928, 1939 and Reticulum. This is the first time that CMDs for NGC 1928 and 1939 have been published. These two CMDs suffer from very dense field star contamination requiring a thorough subtraction algorithm. Using the final CMDs we obtained photometric reddening and metallicity measurements for all three clusters. NGC 1939 is one of the most metal-poor LMC bar clusters, with $[\text{Fe}/\text{H}] = -2.10 \pm 0.19$, while NGC 1928 is significantly more metal-rich, with $[\text{Fe}/\text{H}] = -1.27 \pm 0.14$. Reticulum is of a more intermediate abundance, with $[\text{Fe}/\text{H}] = -1.66 \pm 0.12$. This measurement matches well the previous estimates for this cluster.

All three clusters possess CMDs with features characteristic of the oldest Galactic globular clusters – main sequence turn-offs at $V \sim 23$, and well populated horizontal branches. Both NGC 1928 and 1939 possess very blue HB morphologies, with little or no population stretching to the red of the blue edge of the instability strip. In contrast, Reticulum has a HB populated right across the instability region. To quantify the ages of the three clusters we employed a variety of differential dating techniques, comparing their CMDs to a set of three of the oldest Galactic globular clusters, and three of the oldest LMC globular clusters. We conclude that the entire set of clusters is coeval to within approximately 2 Gyr. This work firmly establishes NGC 1928 and 1939 as members of the LMC globular cluster population, confirming the conclusion obtained by Dutra et al. (1999) from integrated spectroscopy. The LMC globular cluster census therefore now numbers 15, in two distinct groups – the outer clusters NGC 1466, 1841, 2210, 2257, Hodge 11, and Reticulum; and the inner (bar) clusters NGC 1754, 1786, 1835, 1898, 1916, 1928, 1939, 2005, and 2019. The only other LMC cluster older than the lower end of the age gap is ESO121-SC03, at ~ 9 Gyr.

ACKNOWLEDGEMENTS

This paper is based on observations made with the NASA/ESA *Hubble Space Telescope*, obtained at the Space Telescope Science Institute, which is operated by the Association of Universities for Research in Astronomy, Inc., under NASA contract NAS 5-26555. These observations are associated with program 9891. ADM is grateful for financial support from PPARC in the form of a Post-doctoral Fellowship.

REFERENCES

Bica E., Clariá J. J., Dottori H., Santos Jr. J. F. C., Piatti A. E., 1996, *ApJS*, 102, 57
 Brocato E., Castellani V., Ferraro F. R., Piersimoni A. M., Testa V., 1996, *MNRAS*, 282, 614
 Brown T. M., Ferguson H. C., Smith E., Kimble R. A., Sweigart A. V., Renzini A., Rich R. M., VandenBerg D. A., 2003, *ApJ*, 592, L17
 Buonanno R., Corsi C. E., Pulone L., Fusi Pecci F., Bellazzini M., 1998, *A&A*, 333, 505

Burstein D., Heiles C., 1982, *AJ*, 87, 1165
 Chaboyer B., 1999, in Heck A., Caputo F., eds., *Post-Hipparcos Cosmic Candles*. Kluwer, Dordrecht, p. 111
 Dirsch B., Richtler T., Gieren W. P., Hilker M., 2000, *A&A*, 360, 133
 Dolphin A. E., 2000a, *PASP*, 112, 1383
 Dolphin A. E., 2000b, *PASP*, 112, 1397
 Dutra C. M., Bica E., Clariá J. J., Piatti A. E., 1999, *MNRAS*, 305, 373
 Elson R. A. W., Freeman K. C., 1985, *ApJ*, 288, 521
 Elson R. A. W., Fall S. M., 1988, *AJ*, 96, 1383
 Geisler D., Bica E., Dottori H., Clariá J. J., Piatti A. E., Santos Jr. J. F. C., 1997, *AJ*, 114, 1920
 Harris W. E., 1996, *AJ*, 112, 1487
 Holtzman J., et al., 1995, *PASP*, 107, 1065
 Johnson J. A., Bolte M., 1998, *AJ*, 115, 693
 Johnson J. A., Bolte M., Stetson P. B., Hesser J. E., Somerville R. S., 1999, *ApJ*, 527, 199
 Johnson J. A., Bolte M., Stetson P. B., Hesser J. E., 2002, in Geisler D., Grebel E. K., Minniti D., eds., *Proc. IAU Symp. 207, Extragalactic Star Clusters*. Astron. Soc. Pac., San Francisco, p. 190
 Kerber L. O., Santiago B. X., Castro R., Valls-Gabaud D., 2002, *A&A*, 390, 121
 Lee Y.-W., Demarque P., Zinn R., 1994, *ApJ*, 423, 248
 Mack J., et al., 2003, *ACS Data Handbook*, Version 2.0. STScI, Baltimore
 Mackey A. D., Gilmore G. F., 2003a, *MNRAS*, 338, 85
 Mackey A. D., Gilmore G. F., 2003b, *MNRAS*, 338, 120
 Mackey A. D., Gilmore G. F., 2003c, *MNRAS*, 340, 175
 Mackey A. D., Gilmore G. F., 2003d, *MNRAS*, 343, 747
 Mackey A. D., 2004, *PhD Thesis*, Cambridge University
 Marconi G., Ripepi V., Andreuzzi G., Bono G., Buonanno R., Cassisi S., 2002, in Geisler D., Grebel E. K., Minniti D., eds., *Proc. IAU Symp. 207, Extragalactic Star Clusters*. Astron. Soc. Pac., San Francisco, p. 193
 Mateo M., 1987, *ApJ*, 323, L41
 Mighell K. J., Rich R. M., Shara M., Fall S. M., 1996, *AJ*, 111, 2314
 Monelli M., et al., 2003, in Piotto G., Meylan G., Djorgovski S. G., Riello M., eds., *ASP Conf. Ser. Vol. 296, New Horizons in Globular Cluster Astronomy*. Astron. Soc. Pac., San Francisco, p. 388
 Olsen K. A. G., Hodge P. W., Mateo M., Olszewski E. W., Schommer R. A., Suntzeff N. B., Walker A. R., 1998, *MNRAS*, 300, 665
 Rosenberg A., Saviane I., Piotto G., Aparicio A., 1999, *AJ*, 118, 2306
 Riess A., 2003, *ACS Instrument Science Report*, 2003-009
 Sarajedini A., 1994, *AJ*, 107, 618
 Sarajedini A., Forrester W. L., 1995, *AJ*, 109, 1112
 Searle L., Wilkinson A., Bagnuolo W., 1980, *ApJ*, 239, 803
 Suntzeff N. B., Schommer R. A., Olszewski E. W., Walker A. R., 1992, *AJ*, 104, 1743
 VandenBerg D. A., Bolte M., Stetson P. B., 1990, *AJ*, 100, 445
 Walker A. R., 1992, *AJ*, 103, 1166
 Walker A. R., 1993, *AJ*, 106, 999

This paper has been produced using the Royal Astronomical Society/Blackwell Science \LaTeX style file.